**New Physics: Sae Mulli** (The Korean Physical Society), DOI: 10.3938/NPSM.60.375
Volume 60, Number 4, 2010년 4월, pp. 375∼380

# The Structural Study of InN Thin Films Grown on Different Substrates by Using RF Sputtering Method

Weizhen He · Se-Jeong Park
Department of Nano Materials & BK 21 Nano Fusion Technology Division, Pusan National University, Miryang 627-706

Hyung-Kook Kim · Yoon-Hwae Hwang*
Department of Nano Materials & BK 21 Nano Fusion Technology Division, Pusan National University, Miryang 627-706
Research Center For Dielectric and Advanced Matter Physics, Pusan National University, Busan 609-735

Ik-Jae Lee
Pohang Accelerator Laboratory, Pohang University of Science and Technology, Pohang 790-784, Korea

(Received 28 January 2010, in final form 24 March 2010)

We prepared the InN thin films by using RF sputtering on various substrates to investigate the structural characteristics of InN and to find an optimum condition of growing high-quality InN thin film on each substrate. The structural analysis of films deposited on $Al_2O_3$ (0001), Si (100), Pt (200)/$TiO_2$/$SiO_2$/Si, MgO (100) and GaAs (100) is reported by measuring x-ray diffraction and scanning electron microscopy. The InN thin films usually have wurtzite structure. At a certain growth condition, we could get the high quality InN on each substrates except Pt (100). Through atomic force microscopy measurement, it was observed that the InN thin films with c-axis preferred orientation have smoother surface than those with several orientations. It was also found that the thermal expansion coefficient of substrates is also important to get high quality InN thin film.

PACS numbers: 68.55.-a, 68.55.Jk, 81.15.-z, 81.15.Cd
Keywords: InN, Thin film, RF sputtering, c-axis preferred

## I. INTRODUCTION

Nitride semiconductors, especially indium nitrides, have received much attention in the last ten years and this resulted in numerous devices being developed and commercialized. Among the III-nitrides' family, InN has the smallest effective electron mass, the largest mobility, the highest saturation electron drift velocity and overshoot electron velocity [1,2]. These outstanding properties make InN a promising material for applications in high-speed, high-frequency electronic devices [3-8]. Furthermore, the recent studies of InN have corrected its band gap from an earlier value of 1.9eV to 0.6∼0.8eV [9-14], which would expand the applications of the ternary alloys $In_{(1-x)}Ga_xN$ more towards the infrared region. By changing the x value of $In_{(1-x)}Ga_xN$ its band gap could be controlled from the near infrared for InN to the near ultraviolet for GaN [15]. Various growth techniques containing microwave-excited metal/organic vapor phase epitaxy (MEMOVPE), reactive DC or RF sputtering and ion-beam deposition have been studied to obtain the InN thin films.

We did quite a number of studies on the physical properties of hexagonal InN grown on the $Al_2O_3$ (0001) substrate, such as the strain evolution as a function of the film thickness and growth temperature [16], the epitaxial properties and structural relation between hexagonal InN and cubic $In_2O_3$ phases [17] and also the dynamic scaling behavior during the growth stage [18]. However, the lattice mismatch between $Al_2O_3$ and InN is as high as 25.6 % and as we know, the main problem to get high quality InN thin film is the lack of lattice-matched

*E-mail: yhwang@pusan.ac.kr

substrates. Therefore, to find a suitable substrate for growth of InN is also of great importance. In this work we investigated the structural characteristics of InN thin films on several commonly used substrates by using RF sputtering method and found the optimized condition for growing high-quality InN on each substrate.

## II. Experimental

InN films were grown on various substrates by using RF magnetron sputtering method. A two inch-diameter indium metal plate with purity of 99.99 % was used as the target instead of InN. Since indium metal is very soft, we should apply proper RF power to prevent the surface of indium target from a high surface roughness. Based on our preliminary experiments, the RF power was decided to be 20 W, which would not be either too high to destroy the target or too low to reduce the efficiency of deposition. The deposition time and the distance between target and substrate were finally optimized to be 20 min and 5 cm. The substrate temperature should be lower than the decomposition temperature of InN, which is 600 $^{o}$C, and also could not be too low, because low temperature is not good for the formation of crystal. Therefore, the films were deposited at 450 $^{o}$C or 500 $^{o}$C. We grew InN thin films on different substrates, such as $Al_2O_3$ (0001), Si (100), Pt (100), MgO (100), GaAs (100), to observe the substrate dependence of InN structures. The initial pressure of the chamber was $10^{-6}$ torr. Pure $N_2$ gas (purity: 99.999 %) mixed with Ar gas (purity: 99.999 %) was induced during the deposition and the ratio of $N_2$/Ar was varied from 1 to 5 in order to find optimized condition for each substrate. We marked each condition as listed in Table 1.

The structure of the deposited InN films was examined by means of x-ray diffraction (XRD). The XRD measurement was performed at a constant condition for each samples by using a CuK$\alpha$ radiation (wavelength = 1.54056 $\mathring{A}$) and a normal $2\theta/\theta$ scan mode. The scanning electron microscopy (SEM: Model S-4200, HITACHI) and atomic force microscopy (AFM) were also used to analyze the surface morphology.

Table 1. The detail conditions of deposition and the corresponding marks of each conditions.

| Mark of conditions | Gas ratio ($N_2$ : Ar) | Working presure | T | Growth time | RF power |
|---|---|---|---|---|---|
| i | 1 : 1 | 5.26 mtorr | | | |
| ii | 3 : 1 | 10.58 mtorr | 450 $^{o}$C | 20 min | 20 W |
| iii | 5 : 1 | 13.96 mtorr | | | |
| iv | 1 : 1 | 5.26 mtorr | | | |
| v | 3 : 1 | 10.58 mtorr | 500 $^{o}$C | 20 min | 20 W |
| vi | 5 : 1 | 13.96 mtorr | | | |

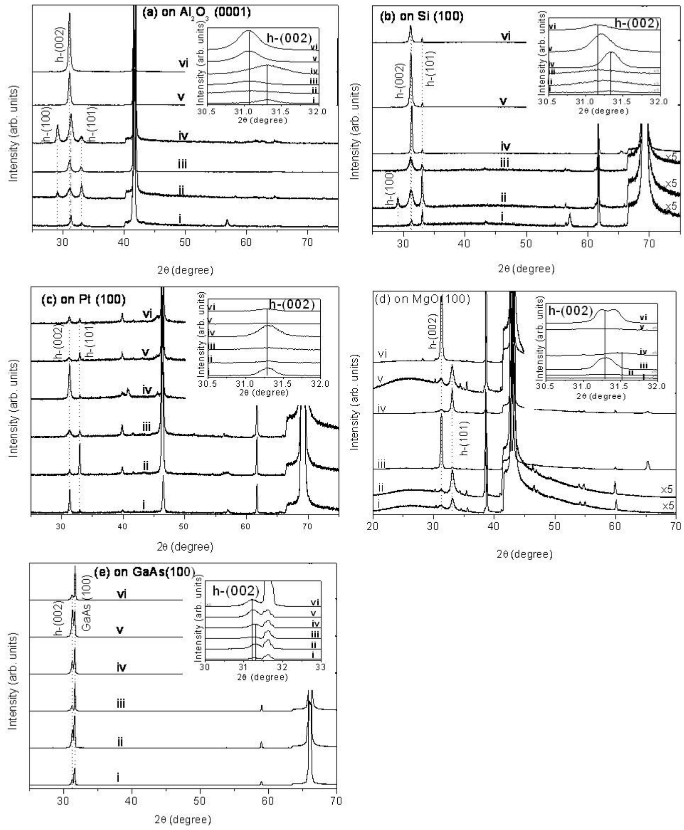


Fig. 1. The XRD patterns of the InN films deposited on (a) $Al_2O_3$ (0001), (b) Si (100), (c) Pt (100), (d) MgO (100) and (e) GaAs (100) at different growth temperatures and $N_2$/Ar ratios.

## III. Results and Discussion

Figure 1 shows the XRD patterns of the InN films deposited on each substrate at different growth conditions. It is obvious that all the peaks appeared in these spectra is associated with hexagonal InN. Therefore we only got wurtzite type InN in our experiments. When we use $Al_2O_3$ (0001) as the substrate (Fig. 1(a)), more than two peaks were detected in the case of conditions (i), (ii), (iii) and (iv), which are hexagonal (002) (h-(002))

peak at around 31.10 $^o$ and h-(101) peak at 33.01 $^o$ or h-(100) peak at 29.11 $^o$. When the InN was deposited at conditions (v) and (vi), only h-(002) peak is observed, which implied that the InN is c-axis preferred oriented. The XRD peak intensity corresponds to the quality of crystalline if all the measurements are carried out at the same condition. The higher intensity of peaks in spectra (iv), (v) and (vi) verified that higher temperature was beneficial to the crystallization. The strongest h-(002) peak in spectrum (v) indicated that the best quality of crystalline of InN could be obtained at the condition (v). The inset is the magnified part where h-(002) peak located. We found that the peak shifted from its origin position to a smaller value. The corresponding lattice constant of c-axis increased from 5.705 $\mathring{A}$ to 5.754 $\mathring{A}$. As we know, when a film is deposited on a substrate whose lattice constants are different from those of the film, the strain between them makes the lattice constants different from the bulk values. It is easier to relax the strain in a polycrystalline structure than in an epitaxial film. Also as the thickness of thin film decreases, the effect of strain is larger. Therefore the strain between substrate and InN makes the lattice of the thin film larger and hence leads the shift of h-(002) peak.

In Fig. 1(b), for the InN grown on Si (100), all the spectra show h-(002) and h-(101) peak. However, h-(002) peak became much stronger while h-(101) evidently weakened as the growth temperature was 500 $^o$C. This means that h-[002] direction is the dominant orientation in the InN films grown on Si (100) at 500 $^o$C. At the condition (v), the InN has a better quality of crystallization than others by judging the peak intensity. In the inset, the same shift of h-(002) peak could be observed as well.

The XRD patterns of InN thin films grown on Pt (100) are shown in Fig. 1(c). The h-(002) and h-(101) peaks appeared in all cases and there's almost no change in the peak intensity when the temperature varied. Here, the increase of temperature gave little influence on the crystallization. As seen in the inset, the position of h-(002) peak doesn't change here. It seems that the strain should have been entirely relaxed in the thin films grown on Pt (100). However, the signal intensity of the $2\theta/\theta$ scan of InN grown on Pt (100) is quite weak indicating a poor crystal quality. Therefore the relaxation of strain should be attributed to the polycrystalline structure of

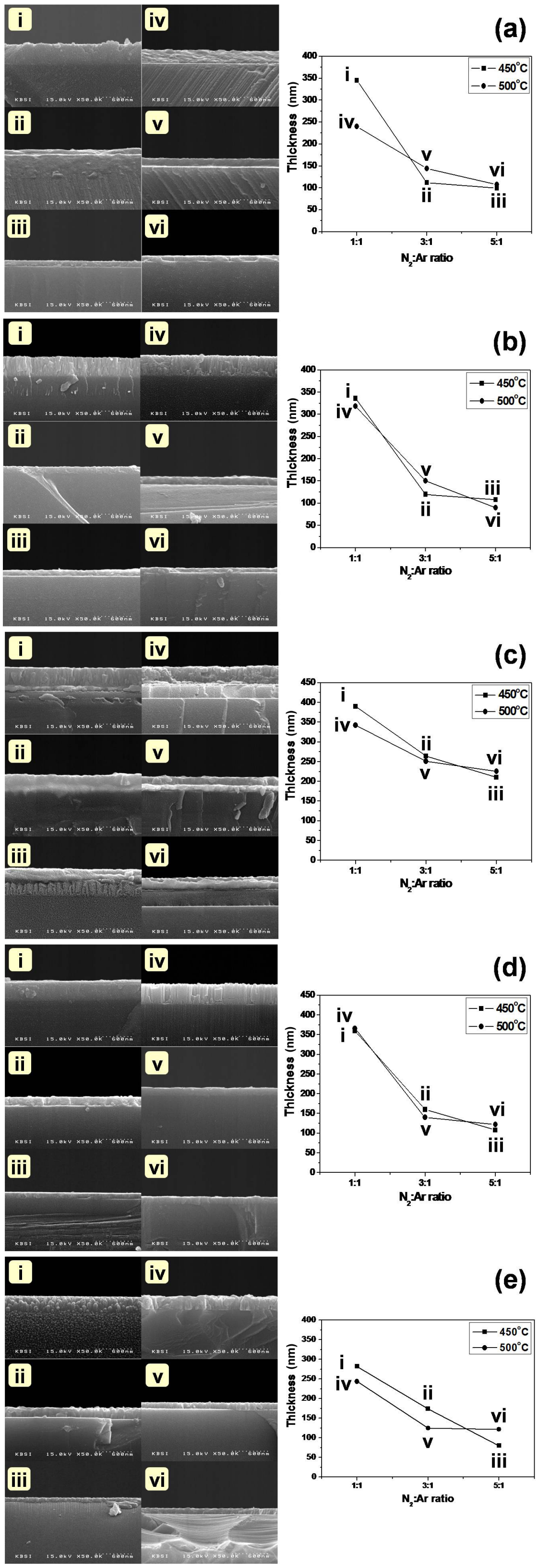


Fig. 2. The cross-section images of InN films grown on a) $Al_2O_3$ (0001), b) Si, c) Pt, d) MgO and e) GaAs substrates (left) and the thickness variation of these films as function of $N_2$/Ar ratio (right).

InN. From the XRD result, Pt (100) is considered as an unsuitable substrate for growing InN.

When we grew InN on MgO (100), we got c-axis preferred InN at conditions (iii) and (vi). Fig. 1(d) shows the XRD patterns of the InN films deposited on MgO (100). The shift of h-(002) peak was observed again, which is resulted from the strain effect.

The XRD spectra are very simple for InN grown on GaAs (100) as shown in Fig. 1(e). The structure of all these films has a preferred orientation of hexagonal [002]. Therefore the GaAs (100) substrate can be a good candidate for the growth of well c-axis oriented hexagonal InN. Furthermore it seems that $N_2$/Ar ratio of 3:1 is the best condition since the peak intensity of InN films deposited at this condition is relatively higher than those in other cases. The position of h-(002) peak also shifted to a smaller value.

To confirm strain effect on the lattice constant, we measured the thickness of these films. Fig. 2 shows cross-section images of InN films grown on each substrates (left) and the thickness variation as function of $N_2$/Ar ratio (right). At lower deposition temperatures, the InN thin films have larger thickness. However, as the $N_2$/Ar ratio increased, the thickness of InN films decreased significantly and finally it is no more than 100 nm. Since the higher gas concentration in sputtering chamber lowered the growth rate and resulted in the decrease in thickness. Considering the XRD result, at conditions (v) and (vi), we got epitaxial InN thin films and here the thicknesses of these two films are much smaller than that deposited at the same temperature but lower $N_2$/Ar ratio, i.e. the condition (iv). Both factors make the strain exist in InN films grown at conditions (v) and (vi) and result the slight change of lattice constant. In the case of conditions (ii) and (iii), although the films are polycrystalline, the sharply decreased thickness leads to the existence of strain between substrate and InN. In the case of using Si (100), Pt (100), MgO (100) or GaAs (100) as substrate, the thickness varies at the same way with that of using $Al_2O_3$ (0001) as substrate. It didn't change much with different growth temperatures but decreased markedly with increasing $N_2$/Ar ratio. The shift of h-(002) peak, i.e. the change of lattice constant, could be explained by considering both the crystalline structure and thickness as presented above.

Table 2. The detail conditions of deposition and the corresponding marks of each conditions.

| Average roughness and the structure of the InN thin films (a for c-axis preferred orientation, b for several orientations) | | | | | | |
|---|---|---|---|---|---|---|
| Condition | 500 $^oC$ | | | | | |
| | 1 : 1 | | 3 : 1 | | 5 : 1 | |
| $Al_2O_3$ (0001) | 2.633 nm | b | 0.5698 nm | a | 0.5885 nm | a |
| Si (100) | 1.217 nm | b | 0.8873 nm | b | 0.9384nm | b |
| Pt (100) | 3.882 nm | b | 2.435 nm | b | 2.358 nm | b |
| MgO (100) | 1.897 nm | b | 1.439 nm | b | 0.8535 nm | a |
| GaAs (100) | 0.3394 nm | a | 0.3739 nm | a | 0.8153 nm | a |

Table 3. Summary of the optimized growth condition for each substrate marked by closed circles.

| Condition | 450 $^oC$ | | | 500 $^oC$ | | |
|---|---|---|---|---|---|---|
| | 1 : 1 | 3 : 1 | 5 : 1 | 1 : 1 | 3 : 1 | 5 : 1 |
| $Al_2O_3$ (0001) | | | | | ○ | |
| Si (100) | | | | | ○ | |
| Pt (100) | Not suitable for growing InN thin film | | | | | |
| MgO (100) | | | | | | ○ |
| GaAs (100) | | | | | ○ | |

The surface roughness was also analyzed by using AFM and the results are listed in Table 2. We also summarized the structure of InN films grown at each condition in the table, and here the letter a stands for c-axis preferred orientation and the letter b stands for several orientations. By comparing the data, we would find that the surfaces of the InN films with the c-axis preferred orientation is smoother than that of those with several orientations. Therefore the c-axis preferred oriented InN thin films also have a better morphologic quality. Based on our findings, we could summarize the optimized condition to grow InN on each substrate and the result is shown in Table 3. As we mentioned, Pt (100) substrate is not suitable for growing InN thin film at all. On most substrates except MgO (100), InN thin films obtained at 500 $^oC$ with gas ratio of 3:1 have the best quality.

Table 4 gives information about the lattice mismatch between the substrates and InN and the thermal expansion coefficient of each substrate material. The lattice mismatch is an important quantity which characterizes epitaxy and is defined as Equation (1):

$$Degree\ of\ mismatch = [a_0(s) - a_0(f)]/a_0(f) \quad (1)$$

where $a_0$(s) and $a_0$(f) refer to the unstrained lattice parameters of substrate and film, respectively. The planes

Table 4. Comparison of lattice mismatch and thermal expansion coefficient $\alpha$ for each substrate with InN.($\alpha$ of InN is 3.8 X $10^{-6}/^{o}C$)

| Substrate | Thermal expansion coefficient | Mismatch with InN (%) |
|---|---|---|
| $Al_2O_3$ (0001) | $7.0 \times 10^{-6}/^{o}C$ | 25.6 |
| Si (100) | $2.3 \times 10^{-6}/^{o}C$ | 30.1 |
| Pt (100) | $9.0 \times 10^{-6}/^{o}C$ | 10.0 |
| MgO (100) | $10.8 \times 10^{-6}/^{o}C$ | 16.0 |
| GaAs (100) | $5.7 \times 10^{-6}/^{o}C$ | 25.1 |

and directions which give the best lattice fit determine the film-substrate orientation. If considering the lattice mismatch only, Pt (100) has the smallest degree of mismatch and it seems that Pt (100) is the best substrate for the growth of a high quality InN thin film. However our experiment results showed opposite result. Therefore we consider another factor, thermal expansion coefficient, $\alpha$.

During heat transfer, the energy that is stored in the intermolecular bonds between atoms changes. When the stored energy increases, so does the length of the molecular bond. As a result, materials typically expand in response to heating. Pt (100) has the best lattice fit but the difference in thermal expansion coefficient is also the largest. In fact, however, $\alpha$ of $Al_2O_3$ and InN also doesn't match so well, therefore we speculate that the difference of $\alpha$ and lattice mismatch work together on the growth of InN. When these two factors work cooperatively it is possible to get high-quality InN growing on $Al_2O_3$. Here "work cooperatively" means that at a high temperature, the thermal expansion effect changed the lattice constant of $Al_2O_3$ and InN as a result of that, the changed lattice constant fit each other. For Pt, the changing in lattice constant by a thermal expansion effect may make their misfit with InN larger and prevent the growth of a high quality InN.

## IV. CONCLUSIONS

In summary, the InN thin films all we obtained by using RF sputtering method have wurtzite structure. At certain conditions, InN with c-axis preferred orientation could be obtained on $Al_2O_3$ (0001), Si (100), MgO (100) and GaAs (100). The Pt (100) substrate is not suitable for growing InN thin film relatively. The thickness of the InN films was independent on the substrate but decreases with increasing the $N_2$/Ar ratio, since the higher gas concentration lowered the growth rate resulting the decreasing in thickness. By considering both the lattice mismatch and difference in thermal expansion coefficient, we proposed that these two factor work together on the growth of InN and when they work cooperatively we could get a high quality InN thin films.

## Acknowledgments

This work was supported for two years by Pusan National University Research Grant

## References

[1] B. E. Foutz, S. K. O'Leary, M. S. Shur and L. F. Eastman, J. Appl. Phys. **85**, 7727 (1999).
[2] S.O'Leary, B. Foutz, M. Shur and L. Eastman, Appl. Phys. Lett. **88**, 152113 (2006).
[3] H. Masataka and M. Toshiaki, J. Cryst. Growth **251**, 494 (2003).
[4] Y. Nanishi, Y. Saito and T. Yamaguchi, Jpn. J. Appl. Phys. **42**, 2549 (2003).
[5] F. H. Yang, J. S. Hwang, Y. J. Yang, K. H. Chen and J. H. Wang, Jpn. J. Appl. Phys. **415**, L1321 (2002).
[6] M. Higashiwaki and T. Matsui, M. Higashiwaki and T. Matsui. **41**, L540 (2002).
[7] E. S. Hwang, E. M. Park, E. K. Suh, C. H. Hong, H. J. Lee, X. Wang and A. Yoshikawa, J. Korean Phys. Soc. **48**, 93 (2006).
[8] E. S. Hwang, E. M. Park, E. K. Suh, C. H. Hong, H. J. Lee, X. Wang, S. B. Che, Y. Shitani and A. Yoshikawa, J. Korean Phys. Soc. **49**, 1530 (2006).
[9] V. Y. Davydov, A. A. Klochikhin, R. P. Seisyan, V. V. Emtsev, S. V. Ivanov, F. Bechstedt, J. Furthmuller, H. Harima, A. V. Mudryi, J. Aderhold, O. Semchinova and J. Graul, Phys. Stat. Sol. B **3**, R1 (2002).
[10] J. Wu, W. Walukiewicz, K. M. Yu, J. W. Ager, E. E. Haller, H. Lu, J. Schaff, Y. Saito and Y. Nanishi, Appl. Phys. Lett. **80**, 3967 (2001).

[11] T. Matsuoka, H. Okamoto, M. Nakao, H. Harima and E. Kurimoto, Appl. Phys. Lett. **81**, 1246 (2002).
[12] Y. Saito, H. Harima, E. Kurimoto, T. Yamaguchi, N. Teraguchi, A. Suzuki, T. Araki and Y. Nanishi, Phys. Stat. Sol. B **234**, 796 (2002).
[13] M. Hori, K. Kano, T. Yamaguchi, Y. Saito, T. Araki, Y. Nanishi, N. Teraguchi and A. Suzuki, Phys. Stat. Sol. B **234**, 750 (2002).
[14] J. W. Yoon, S. S. Kim, H. Cheong, H. C. Seo, S. Y. Kwon, H. J. Kim, Y. Shin, E. Yoon and Y. S. Park, J. Korean Phys. Soc. **49**, 2143 (2006).
[15] J. Wu, W. Walukiewicz, K. M. Yu, J. W. Ager III, E. E. Haller, Hai Lu and William J. Schaff, Appl. Phys. Lett. **80**, 4741 (2002).
[16] T. B. Hur, I. J. Lee, J. W. Kim, Y. H. Hwang and H. K. Kim, Jpn. J. Appl. Phys. **41**, 1932 (2002).
[17] T. B. Hur, I. J. Lee, H. L. Park, Y. H. Hwang and H. K. Kim, Solid State Communications **130**, 397 (2004).
[18] I. J. Lee, J. W. Kim, T. B. Hur, Y. H. Hwang and H. K. Kim, Appl. Phys. Lett. **81**, 475 (2002).